TES microcalorimeter detectors suitable for neutrino mass measurement

Andrea Giachero

University & INFN of Milano-Bicocca

EUCAS 2019
GLASGOW

Scientific case: measurement of the neutrino mass

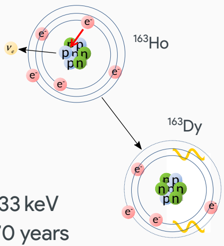

$Q_{EC} = 2.833$ keV
$\tau_{1/2} \simeq 4570$ years

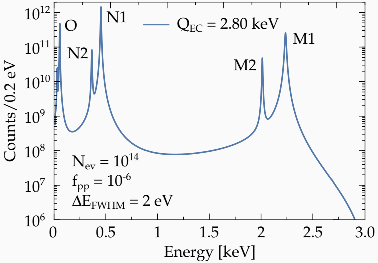

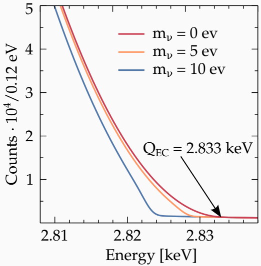

- Electron capture from shell $\geq$ M1 $\Rightarrow$ $^{163}\mathrm{Ho} + e^- \rightarrow {}^{163}\mathrm{Dy}^* + \nu_e(E_c)$;
- End-point shaped by $\sqrt{(Q - E_e)^2 - m_\nu^2}$ (the same of the β-decay);
- Searching for a tiny deformation caused by a non-zero neutrino mass to the spectrum near its end point;
- Calorimetric measurement of Dy atomic de-excitations (mostly non-radiative)

  $\Rightarrow$ measurement of the entire energy released except the ν energy;

proposed for the first time
by A. De Rujula e M. Lusignoli in 1982
Phys. Lett. 118B (1982) 429
Nucl. Phys. B219 (1983) 277-301

more details on A. Nucciotti
Adv. High En. Phys. 2016 (2016) 9153024
and M. Galeazzi *et al.*
arXiv:1202.4763 [physics.ins-det]

The HOLMES experiment (ERC-2013-AdG no. 340321)

The statistical sensitivity $\Sigma(m_\nu)$ has:

- Strong dependence on statistic: $\Sigma(m_\nu) \propto N_{events}^{1/4}$
- Strong dependence on rise time pile-up: $f_{pp} \simeq A_{EC} \cdot \tau_{res}$

  Pulse pile-up occurs when multiple events arrive within the temporal resolving time of the detector (i.e. $E_1 + E_2 = Q_{EC}$);

  (A_{EC}: pixel activity, τ_{res}: time resolution)
- Weak dependence on energy resolution ΔE;

Large arrays of fast detectors are a fundamental requirements

HOLMES target

- Microcalorimeters base on Transition Edge Sensors with ^{163}Ho implanted Au absorber;
- Pixel activity of $A_{EC} \sim 300$ Bq/det;
- Energy resolution: O(eV)
- Time resolution: $\tau_{res} \sim 3\ \mu s$ ($\tau_{rise} = 10 - 20\ \mu s$);
- 1000 channels for $3 \cdot 10^{13}$ events collected in $T_M = 3$ years;
- Expected Sensitivity: $m_\nu \leq 2$ eV

more details on Eur. Phys. J. C (2015) 75: 112

Pile-up Spectrum

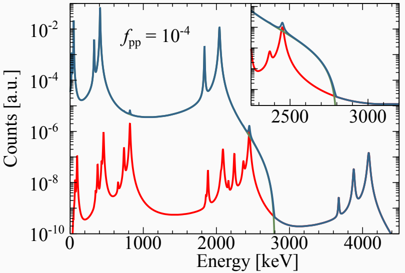

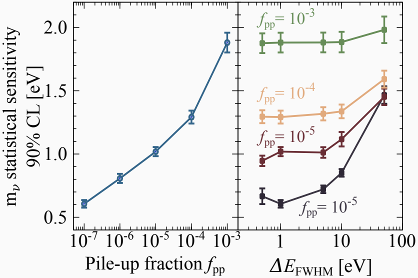

HOLMES: TES-based microcalorimeters

Microcalorimeters

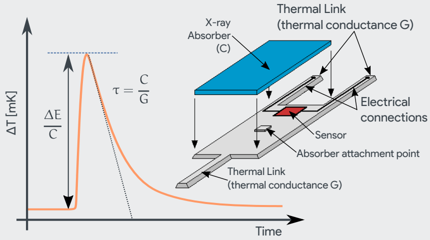

The X-ray microcalorimeter works by sensing the heat generated by X-ray photons when they are absorbed and thermalized in a very low heat capacity element.

- Absorber:
  - Very low thermal capacity (small size, $T < 100$ mK);
  - High stopping power (high Z material).
- Sensor:
  - Si or Ge Thermistors, TES, MMC, ...

Transition Edge Sensor (TES)

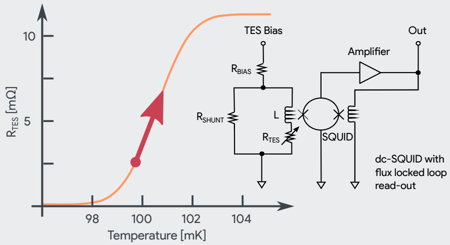

- Exploits strongly temperature-dependent resistance of the superconducting phase transition;
- Low resistance: read out with SQUIDs (Superconducting Quantum Interference Devices);
- Small size, low thermal capacity, excellent energy resolution $\Delta E \simeq 1$ eV @ 1.5 keV;
- Large array and multiplexing (TDM, CDM , FDM and μwave) (more details on the Joel Ullom presentation);

HOLMES

<presentation:0>

Worst background: 2 x-ray events analyzed as 1 with a total energy around $Q_{EC} \Rightarrow$ pile-up events

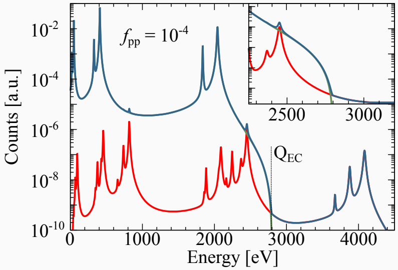

The ^{163}Ho pile-up events spectrum is quite complex and presents a number of peaks right at the end-point of the decay spectrum;

$$S(E_c) = \left[N_{ev}(N_{EC}(E_c, m_\nu) + f_{pp} \times N_{EC}(E_c, 0) \otimes N_{EC}(E_c, 0)) + B(E_c)\right] \otimes R_{\Delta E}(E_c)$$

- A_{EC} : decay activity
- $f_{pp} = A_{EC} \times \tau_r$: pile-up rate
- $S(E_c)$: total theoretical spectrum
- $N_{EC}(E_c, m_\nu)$: ^{163}Ho spectrum
- $B(E)$: background energy spectrum
- $R_{\Delta E}(E_c)$: detector energy response function

more details on Eur. Phys. J. C 74 (2014) 3161

- Pulse pile-up occurs when multiple events arrive within the temporal resolving time of the detector (i.e. $E_1 + E_2 = Q_{EC}$);
- Unresolved pile-up at the end-point Q_{EC} produces a sort of background close to the end-point;
- To resolve pile-up:
  - Detector with high time resolution τ_r (and fast signal rise-time τ_{rise});
  - Efficient pulse pile-up recovery algorithm (Wiener filter, Singular Value Decomposition)
- The classical multiplexing schemas (TDM, CDM and FDM) provides a limited multiplexing factor (<40) and limited bandwidth (few MHz) on single detector $\Rightarrow$ new approach: microwave multiplexing

HOLMES: TESs design

4 × 16 sub-array

Singe Pixel

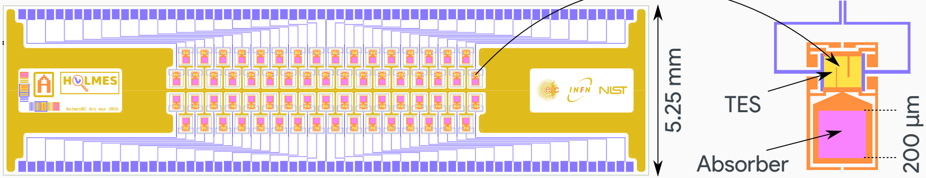

- Sensor: TES Mo/Au bilayers, critical temperature $T_c = 100$ mK;
- Absorber: Gold, 2 μm thick for full e/γ absorption;
- Side-car design to avoid TES proximitation;
- Thermal conductance G engineering for τ_{decay} control;
- 4 $\times$ 16 linear sub-array designed for high implant efficiency;
- Optimized design for high speed and high resolution:

Single Pixel
(real photo)

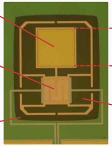

$$@3\,\text{keV}: \Delta E_{FWHM} \simeq 3-4\,\text{eV}, \; \tau_{rise} \simeq 10\,\mu\text{s}, \; \tau_{decay} \simeq 100\,\mu\text{s}$$

^{163}Ho isotopes embedded in metallic absorbers (through ion-implantation)

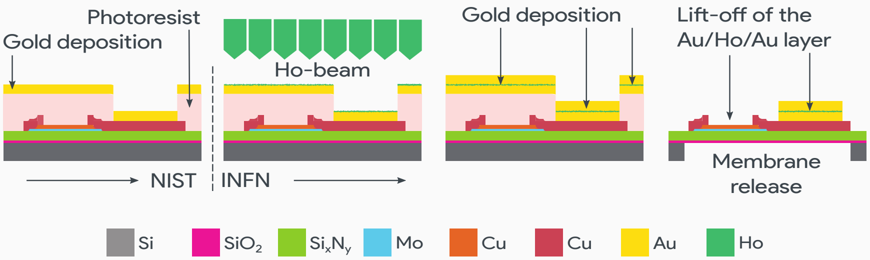

- Fabrication in two steps:
  - NIST: Au absorber bottom-part placed side-by-side with the Mo/Cu sensor on a silicon nitride;
  - INFN: Au absorber finalized into the implanter deposition chamber during the ^{163}Ho implanting procedure;
- SiN membrane release by Silicon Deep Reactive Ion Etching (DRIE) or Silicon KOH anisotropic wet etching
  $\Rightarrow$ tests currently in progress;
- 2 μm thick Au encapsulating implanted Ho;

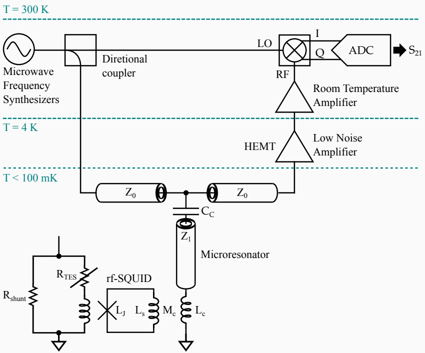

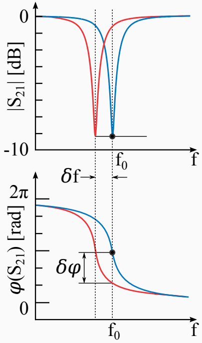

- dc-biased TES inductively coupled to a dissipationless rf-SQUID;
- rf-SQUID inductively coupled to a high-Q superconducting $\lambda/4$ resonator;
- Change in TES current $\Rightarrow$ change in the input flux to the SQUID;
- Change in the input flux to the SQUID $\Rightarrow$ change of resonance frequency and phase;
- Each micro-resonator can be continuously monitored by a probe tone;

Microwave rf-SQUID multiplexing (cont.)

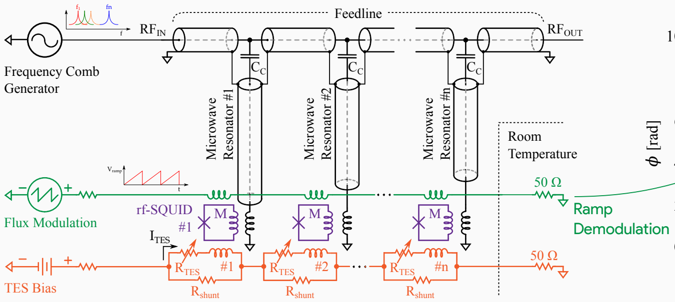

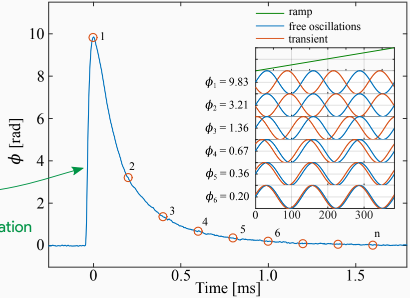

- By coupling many resonators to a single microwave feedline it is possible to perform the readout of multiple detectors
- Sensors are monitored by a set of sinusoidal probe tones (frequency comb);
- At equilibrium, the resonator frequencies are matched to the probe tone frequencies, and so each resonator acts as a short to ground;
- The ramp induces a controlled flux variation in the rf-SQUID, which is crucial for linearizing the response;
- Large multiplexing factor ($>$ 100) and bandwidth, currently limited by the digitizer bandwidth.

The Multiplexing chip

The core of the microwave multiplexing is the multiplexer chip

Designed and developed by NIST

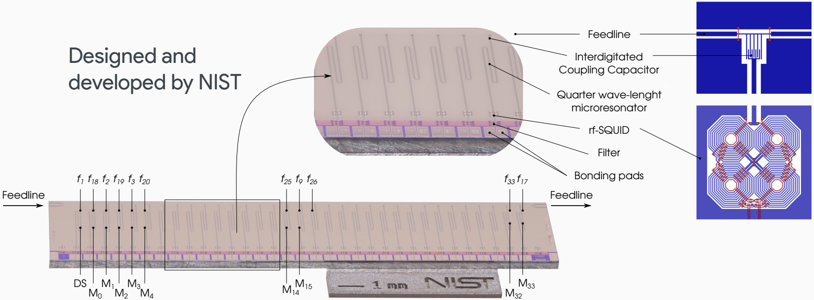

- Superconducting 33 quarter-wave coplanar waveguide (CPW) microwave resonators;
- 200 nm thick Nb film deposited on high-resistivity silicon ($\rho > 10$ kΩ·cm);
- Each resonator has a trombone-like shape with slightly different length;
- The SQUID loop is a second order gradiometer consisting of four parallel lobes;
- Wiring in series different 33-channel chips with different frequency band allows to increase the multiplexing factor (daisy chain)

Microwave readout hardware implementation

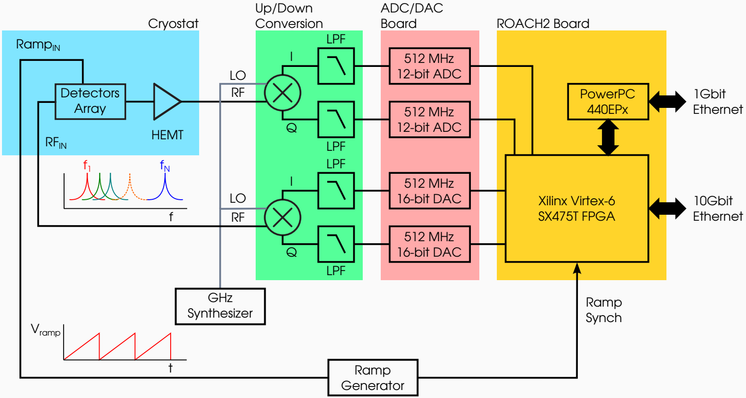

- A key enabling technology for large-scale microwave multiplexing is the digital approach;
- This allows to exploit standard software-defined radio (SDR) used in microwave-frequency communication.
- Open architecture computing hardware ROACH2 (Reconfigurable Open Architecture Computing Hardware) as FPGA processing board;

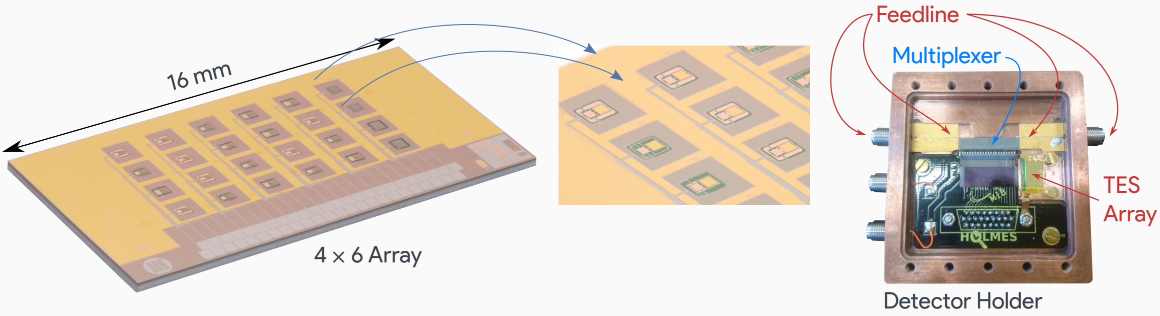

- Sensor: TES Mo/Au bilayers, critical temperature $T_c = 100$ mK;
- Absorber: Gold, 2 μm thick for full e^- / γ absorption (sidecar design);
- First 4×6 array prototype produced at NIST and tested in Milano with μwave-readout;
- Different Perimeter/Absorber configurations in order to study the detector response;

HOLMES: the multiplexer chips (μmux17a)

Forward transmissiom S_{21} of 4 different band chips wired in series

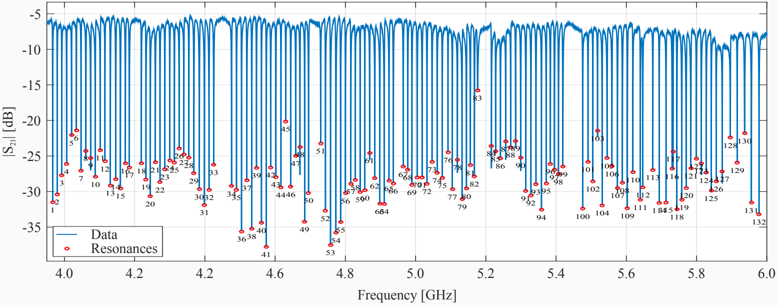

Example of resonance fit

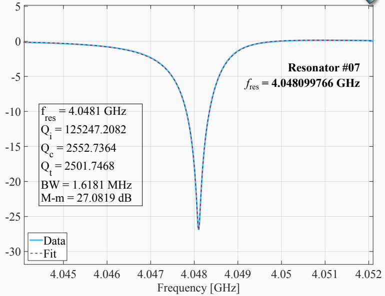

		Required	Measured
Resonators bandwidth	Δf_{BW} [MHz]	2	2 ± 1
Resonators spacing	Δf [MHz]	14	14 ± 1
Resonators depth	ΔS [dB]	> 10	29 ± 6

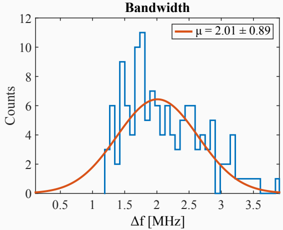

All the microresonator parameters match the HOLMES specification

HOLMES multiplexing readout: current status

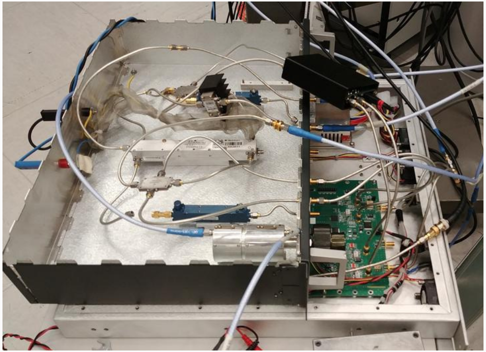

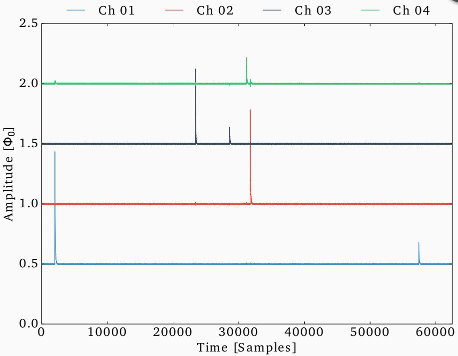

- ROACH2 board for tones generation/acquisition and for digital processing;
- Custom intermediate frequency (IF) circuitry for up/down conversion;
- Working with: $n_{\Phi_0} = 2$, $f_{\text{ramp}} = 500\,\text{kHz}$, $f_{\text{ADC}} = 512,\text{MHz}$
- 16-channel firmware from NIST (uses only half of available ADC bandwidth);
- 4 pixels measurements $\Rightarrow$ limited by available tone power;

HOLMES: detectors characterization with a fluorescence source

HOLMES

Event pulses due to the chlorine x-rays

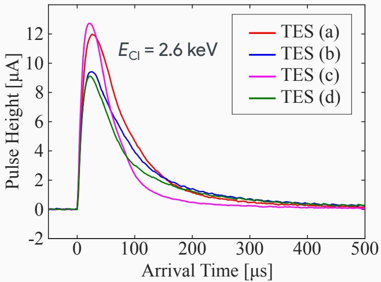

Uncalibrated energy spectra

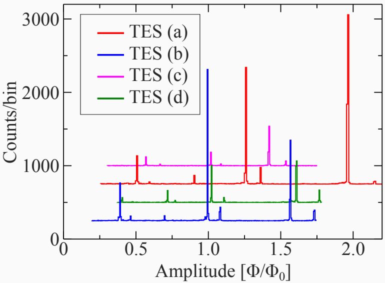

Second order calibration curve $\Phi_0 \longleftrightarrow$ keV

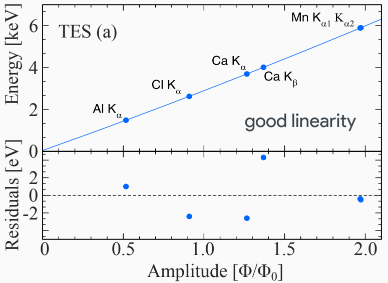

- Detectors characterization on non implanted detectors;
- Tests on four different detector designs;
- Calibration run performed with a primary ^{55}Fe source faced to different target
- x-ray fluorescence emission lines:

  ^{55}Mn (5.9 keV) ^{40}Ca (3.7 keV)
  ^{40}Cl (2.6 keV) ^{27}Al (1.5 keV)

more details on
Eur. Phys. J. C (2019) 79:304

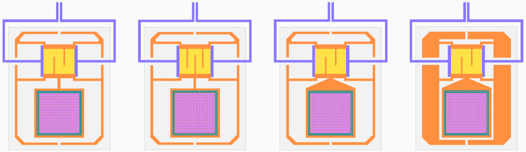

TES (a) TES (b) TES (c) TES (d)

HOLMES

Separation of the $K_{\alpha 1}$ and $K_{\alpha 2}$ of the Mn

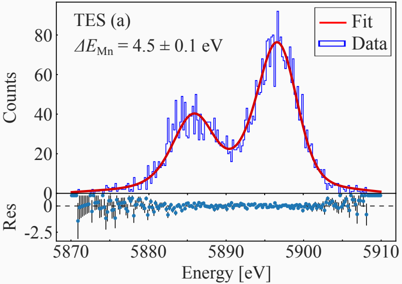

Measured noise power spectral density compared with the theoretical model

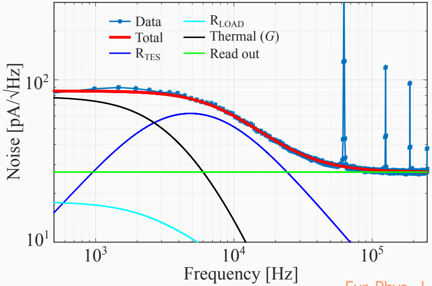

more details on Eur. Phys. J. C (2019) 79:304

4 detector satisfied the HOLMES requirements ⇒ For the best detector: $\Delta E_{Mn} = 4.5 \pm 0.3$ eV @ 2.6 keV

TES #	ΔE_{Al} [eV] (1486 eV)	ΔE_{Cl} [eV] (2622 eV)	ΔE_{Ca} [eV] (3691 eV)	ΔE_{Mn} [eV] (5899 eV)	τ_{rise} [μs] (2622 eV)	τ_{short} [μs] (2622 eV)	τ_{long} [μs] (2622 eV)
2 (b)	8.6 ± 0.3	8.8 ± 0.7	7.8 ± 0.2	8.3 ± 0.3	11	56	220
6 (d)	6 ± 1	6.0 ± 0.4	6.4 ± 0.4	6.2 ± 0.4	12	34	170
8 (a)	4.5 ± 0.3	5.0 ± 0.5	5.0 ± 0.2	4.5 ± 0.1	13	54	220
11 (c)	4.3 ± 0.3	4.5 ± 0.3	4.6 ± 0.3		14	32	180

Measured read out noise

$$n_s = (2-3)\ \mu\Phi_0/\sqrt{\mathrm{Hz}}$$
$$\sim (23-35)\ \mathrm{pA}/\sqrt{\mathrm{Hz}}$$

HOLMES: next steps

Version designed to release the membrane with KOH

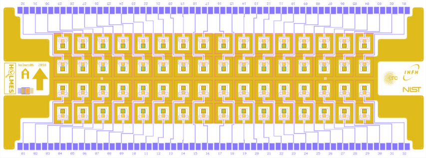

Version designed to release the membrane with DRIE

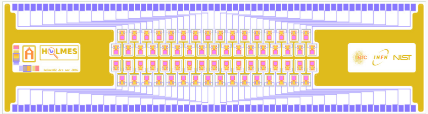

- 2^{nd} detectors generation in production at NIST
  - 4×16 linear sub-array designed for high implant efficiency;
  - First production with sensor/absorber with few differences for determining the better pixel baseline;
  - Second production with pixel baseline implemented and with ^{163}Ho-implanted absorber;
- 4 multiplexer chips with different bandwidht produced at NIST and ready to be send in Milano;
- 64-channel read out and multiplexing system development started in 2019;
  - Based on the 2 ROACH2 systems ($f_{ADC} = 512$ MHz)
  - Semicommercial up/down converter system able to drive 32 microresonator/board
- ^{163}Ho implanted activity optimized before the end of 2019
  - first high ^{163}Ho activity array running in 2020
  - 1 month of 2 (4×16)-sub array data taking can provide a statistical sensitivity $m_\nu \leq 10$ eV

Conclusion

HOLMES

- The measurement of the end point of nuclear beta or electron capture (EC) decays spectra is the only model-independent;
- The goal of the next future experiments is the sub-eV neutrino mass sensitivity;
- TES x-ray microcalorimeters have already demonstrated high resolution and fast response $\Rightarrow$ large array of these detectors are suitable for the direct measurement of neutrino mass;
- The HOLMES experiment will performe a direct measurment of the neutrino mass by using microcalorimenters with absorber ^{163}Ho-implanted
  - 100 MBq of ^{163}Ho produced $\Rightarrow$ enough for R&D and 512 pixels;
  - First ^{163}Ho implanting in array absorber running in 2020;
  - 64-channel read out and multiplexing system ready at the end of 2019;
- First physics measurement from the first two sub-array foreseen from 2020;
- Final 1024-pixel configuration will follow;